A retentive memory of tetrachloroethene respiration in *Sulfurospirillum halorespirans* - involved proteins and a possible link to acetylation of a two-component regulatory system

Dominique Türkowsky[§,1], Jens Esken[2,§], Tobias Goris[2], Torsten Schubert[2], Gabriele Diekert[2], Nico Jehmlich[1], Martin von Bergen[1,3]

[1]Department of Molecular Systems Biology, Helmholtz Centre for Environmental Research – UFZ, Permoserstraße 15, 04318 Leipzig, Germany

[2]Department of Applied and Ecological Microbiology, Institute of Microbiology, Friedrich Schiller University, Philosophenweg 12, 07743 Jena, Germany

[3]Institute of Biochemistry, Faculty of Life Sciences, University of Leipzig, Brüderstraße 34, Germany

[§]These authors contributed equally to this work

Correspondence:

Prof. Dr. Martin von Bergen

E-mail: martin.vonbergen@ufz.de, Tel: +49-341-235-1211

Abstract

Organohalide respiration (OHR), comprising the reductive dehalogenation of halogenated organic compounds, is subject to a unique memory effect and long-term transcriptional downregulation of the involved genes in *Sulfurospirillum multivorans*. Gene expression ceases slowly over approximately 100 generations in the absence of tetrachloroethene (PCE). However, the molecular mechanisms of this regulation process are not understood. We show here that *Sulfurospirillum halorespirans* undergoes the same type of regulation when cultivated without chlorinated ethenes for a long period of time. In addition, we compared the proteomes of *S. halorespirans* cells cultivated in the presence of PCE with those of cells long- and short-term cultivated with nitrate as sole electron acceptor. Important OHR-related proteins previously unidentified in *S. multivorans* include a histidine kinase, a putative quinol dehydrogenase membrane protein, and a PCE-induced porin. Since for some regulatory proteins a posttranslational regulation of activity by lysine acetylations is known, we also analyzed the acetylome of *S. halorespirans*, revealing that 32% of the proteome was acetylated in at least one condition. The data indicate that the response regulator and the histidine kinase of a two-component system most probably involved in induction of PCE respiration are highly acetylated during short-term cultivation with nitrate in the absence of PCE.

Significance

The so far unique long-term downregulation of organohalide respiration is now identified in a second species suggesting a broader distribution of this regulatory phenomenon. An improved protein extraction method allowed the identification of proteins most probably involved in transcriptional regulation of OHR in *Sulfurospirillum* spp. Our data indicate that acetylations of regulatory proteins are involved in this extreme, sustained standby-mode of metabolic enzymes in the absence of substrate. This first published acetylome of Epsilonproteobacteria might help to study other ecologically or medically important species of this clade.

Highlights

- First integrated omics approach including proteomics and acetylomics of an Epsilonproteobacterium

- Systematic comparison of protein production and regulatory mechanisms in organohalide respiration
- Improved protein extraction allowed higher coverage of membrane proteins
- Lysine acetylations within the two-component regulatory system might be involved in long-term downregulation

Keywords

Regulation; two-component regulatory system; acetylomics; proteomics; bioremediation; dehalorespiration

Introduction

The anaerobic respiration with halogenated compounds, called organohalide respiration (OHR), is of importance for bioremediation and the global halogen cycle. OHR relies on a reductive dehalogenase as terminal reductase [1]. The molecular mechanisms underlying OHR, including its regulation, is unresolved to a great extent. The Epsilonproteobacterium *Sulfurospirillum multivorans* is able to reductively dehalogenate the environmentally harmful but widely distributed degreasing agent tetrachloroethene (PCE) to *cis*-dichloroethene. This is catalyzed by the PCE reductive dehalogenase (PceA). When *S. multivorans* is cultivated in the absence of PCE, PceA is subject to a memory effect: PceA is still produced, but during a long-term downregulation gene expression ceases slowly within approximately 100 generations [2]. A similar long-term loss of PCE respiration was observed in *Desulfitobacterium hafniense* strains Y51, PCE-S, and TCE1 [3-5]. However, in these *D. hafniense* strains, the loss of PCE respiration was not due to a regulatory effect but a transposon-mediated loss of the *pce* gene cluster in the majority of the bacterial population after cultivation in the absence of PCE [3, 5]. In *S. multivorans*, the *pceA* gene is still present after long-term cultivation without PCE but is not transcribed anymore [2]. The *pceA* transcription can be induced again by PCE. The *pceA* gene of *S. multivorans* is embedded in a large gene region encoding putative electron-transfer proteins for the PCE respiratory chain and proteins necessary for the production of its cobamide cofactor (norpseudo-B_{12}) [6]. Evidence was obtained that this gene region undergoes concerted, PCE-induced transcriptional regulation [6, 7]. Until recently, *S. multivorans* was the only organohalide-respiring Epsilonproteobacterium with a sequenced genome, hindering global comparisons of PCE respiration

and its regulation on a genetic basis so far. Therefore, the genome of a second PCE-respiring Epsilonproteobacterium, *Sulfurospirillum halorespirans*, was sequenced and described [8]. Overall, both organisms show similar genome features, although unlike *S. multivorans* and unusual for an organohalide-respiratory bacterium, *S. halorespirans* harbors *nos* and *sox* proteins, involved in nitrous oxide respiration and thiosulfate oxidation, respectively. The OHR gene region of *S. halorespirans* displays nearly 100% nucleotide sequence identity compared to *S. multivorans* with three exceptions: (1) The *pceA* gene is only 95% identical to that of *S. multivorans*, (2) 106 nucleotides that might contain a small ORF are present upstream of the norpseudo-B_{12} (*cbi*) biosynthesis gene cluster in *S. halorespirans* and (3) an intact *tetR*-like repressor gene downstream of this *cbi* cluster is interrupted by a transposase in *S. multivorans*. The latter two features and a PceA with an even lower degree of sequence identity distinguish also the OHR regions of the recently sequenced *Sulfurospirillum* sp. JPD-1 (accession number CP023275) and Candidatus *Sulfurospirillum diekertiae* [9] from *S. multivorans*. Further regulators encoded in the OHR region of both organisms are two two-component regulatory systems (TCSs). The first, TCS I, is located downstream of *pceAB*. A second, similar TCS, TCS II, is encoded downstream of a second reductive dehalogenase gene set (*rdhAB*). Both TCSs are formed by two multidomain proteins, a histidine protein kinase (HK) and a response regulator (RR). The HKs consist of a periplasmic N-terminal domain putatively involved in ligand binding, a transmembrane domain with seven transmembrane helices, a dimerization/histidine phosphotransfer domain and a catalytic and ATP-binding domain [6]. The RRs harbor a receiver domain as well as a winged helix turn helix (HTH) motif and might be involved in transcriptional activation of the OHR regulon. The role of the second reductive dehalogenase is up to now unknown and its expression was never observed regardless of the substrate tested [7]. However, the TCS II was described as a candidate for PCE-sensing, because the RR (SMUL_1539) was detected in the proteome of *S. multivorans* cells cultivated with and without PCE [7], which is opposed to the TCS I, which has never been detected in proteome studies. Besides OHR region genes, the expression of which was highly upregulated by PCE, only a few genes in *S. multivorans* were found to undergo regulation in the presence of PCE. Among them, stress-induced proteins such as an Hsp20 family protein might play a role in a specific stress response in *S. multivorans* [7].

The trigger which retains expression of the OHR-related genes in the absence of PCE is still unknown. Post-translational modifications (PTMs) of proteins are important regulators, but their role has been

underestimated in bacteria for a long time. One important PTM in bacteria with diverse functions is the acetylation of proteins. Proteins get reversibly modified by an interplay of acetyltransferases and deacetylases or non-enzymatically by acetylphosphate [10]. By neutralizing the positive charge of lysine, acetylations may alter local or global protein structure, which can have an impact on the protein's stability, activity, localization or interaction with other proteins and other biomolecules. In bacteria, these processes were observed to play a role e.g. in the regulation of cell motility and shape, RNA degradation and gene expression [10].

The aim of our study was to show that the long-term downregulation of OHR is present in another *Sulfurospirillum* sp. and to get insight into its regulation by analyzing the proteome during different stages of the long-term downregulation. We hypothesized that lysine acetylations could play a role in the delay of downregulation in *Sulfurospirillum* species.

Methods

Cultivation of *S. multivorans*

S. halorespirans DSM 13726 (PCE-M2) was cultivated anaerobically at 28°C in a defined mineral medium [11] in the absence of exogenous cobamide and yeast extract. Pyruvate (40 mM) was used as electron donor and nitrate (40 mM) or PCE as electron acceptor. PCE was added to the medium (10 mM nominal concentration) from a hexadecane stock solution (0.5 M). In order to generate *S. halorespirans* cells with down-regulated *pceA* gene expression [2], the organism was cultivated for 60 transfers (10% inoculum each) with nitrate as sole electron acceptor (Fig. 1). The inoculum corresponded to about 6 µg protein per mL medium. Each cultivation was performed in 100 mL glass serum bottles. For proteomic analyses, cells were cultivated in 1 L or 500 mL medium in rubber-stoppered 2 L or 1 L glass bottles, respectively. Cells were harvested during early (OD_{578} ≈ 0.11) and late (OD_{578} ≈ 0.20) exponential phase. The ratio of aqueous to gas phase was always 1:1. The bacterial growth was monitored photometrically by measuring the optical density at 578 nm. All cultivations were performed in triplicates.

Cell harvest, disruption and PceA activity assay

S. halorespirans cells were harvested from a 100 mL culture in the late exponential growth phase by centrifugation (12,000 x g, 10 min at 10°C). Cell pellets were washed three times with 50 mM Tris-HCl (pH 7.5) to ensure the removal of PCE and nitrate. The cell pellets were transferred into an anoxic glove box and resuspended (1:2) in anoxic buffer (50 mM Tris-HCl, pH 7.5). An equal volume of glass beads (0.25–0.5 mm diameter, Carl Roth GmbH, Karlsruhe, Germany) was added and the cells were disrupted using a bead mill (5 min at 25 Hz; MixerMill MM400, Retsch GmbH, Haan, Germany). The crude extracts were separated from the glass beads by centrifugation (14,000 x g, 2 min) under anoxic conditions. The measurements of PceA activity were performed as described using a photometric assay with reduced methyl viologen as artificial electron donor [12].

Immunoblot analysis

Cells were harvested as described above. Protein concentration was determined using the Bio-Rad Bradford reagent (Bio-Rad, Munich, Germany) and bovine serum albumin as a protein standard. Soluble fractions (10 µg protein per lane) were subjected to denaturing SDS-PAGE (12.5%) and afterwards blotted onto a polyvinylidene difluoride (PVDF) membrane (Roche, Mannheim, Germany) using a semi-dry transfer cell (Bio-Rad, Munich, Germany) according to the protocol described by John *et al.* (2009) [2]. The PceA antiserum (primary antibody) was diluted 500,000-fold. The primary antibody was detected via a secondary antibody (diluted 1:30,000) coupled to alkaline phosphatase (Sigma-Aldrich, Munich, Germany).

Structural modeling of the two-component system

The structural models of the cytoplasmic domain of the HK and the RR were generated using the I-TASSER server for protein structure and function prediction [13, 14]. The best threading templates used by the platform were the HK KinB of *Geobacillus stearothermophilus* with the inhibitor Sda (PDB ID 3D36, [15]) and the RR MtrA of *Mycobacterium tuberculosis* (PDB ID 2GWR, [16]). The acetylations were added to the structural model using the PyTMs plugin [17] of the PyMOL Molecular Graphics System [18].

Peptide preparation from lysed cells

S. halorespirans cells were harvested in the early (OD_{578} ≈ 0.11) and late (OD_{578} ≈ 0.20) exponential growth phases by centrifugation (12,000 x g, 10 min at 10°C). The cell pellets were washed once in PBS buffer (140 mM NaCl, 10 mM KCl, 6.4 mM Na_2PO_4, and 2 mM KH_2PO_4). Protein extraction, digestion, and peptide purification were performed as described before [19]. Briefly, cells were dissolved in 8 M urea lysis buffer (20 mM HEPES, 8M urea, 1 mM sodium vanadate, 1 mM β-glycerolphosphate, 2.5 mM sodium pyrophosphate) and lysed by four cycles of freeze/thaw/ultrasonic bath treatment. Cell debris was removed by centrifugation (15 min, 4 °C, 20,000 g), proteins were quantified by BCA-assay (Thermo Fisher Scientific, USA), reduced (4.5 mM dithiothreitol, 30 min, 55 °C) and alkylated (10 mM iodoacetamide, 15 min, room temperature, in the dark). Samples were diluted four-fold with 20 mM HEPES, pH 8, and 5.3 mg was digested overnight with 20 µg trypsin (Promega) and subsequently with 3.5 µg lysyl endopeptidase (Wako, Japan) for six hours. Digested peptides were acidified with 1% trifluoroacetic acid (TFA), desalted over SEP PAK Classic C18 columns (Waters, USA) and eluted using 40% acetonitrile in 0.1% TFA. 5% of the eluate was aliquoted for the proteome analysis; all samples were lyophilized and stored at -80°C.

Immunoaffinity enrichment of lysine-acetylated peptides

Enrichment of acetylated peptides was conducted using the PTMScan Acetyl-Lysine Motif Kit (Cell Signaling Technology, USA) as described in [19]. Peptides were dissolved in IAP buffer and incubated with the antibody beads for 2 h at 4 °C. The beads were washed with IAP buffer and water and the peptides were eluted in two steps with 0.15% TFA. Non-modified and acetylated peptides were desalted by using C18 Zip Tip columns (Millipore, Germany), dissolved in 0.1% formic acid and injected into a liquid chromatography tandem mass spectrometer (LC-MS/MS).

Mass spectrometry

Separation of tryptic peptides was performed using a 120 min non-linear gradient from 3.2% to 40% acetonitrile, 0.1% formic acid on a C18 analytical column (Acclaim PepMap100, 75 µm inner diameter, 25 cm, C18, Thermo Scientific) in a UHPLC system (Ultimate 3000, Dionex/Thermo Fisher Scientific, Idstein, Germany). Mass spectrometry was performed on a Q Exactive HF MS (Thermo Fisher Scientific, Waltham, MA, USA) with a TriVersa NanoMate (Advion, Ltd., Harlow, UK) source in LC chip

coupling mode. Mass spectrometer full scans were measured in the Orbitrap mass analyzer within the mass range of 400–1,600 *m/z*, at 60,000 resolution using an automatic gain control target of 3×10^6 and maximum fill time of 50 ms. An MS/MS isolation window for ions in the quadrupole was set to 1.4 *m/z*. MS/MS scans were acquired using the higher energy dissociation mode at a normalized collision-induced energy of 28%, within a scan range of 200–2,000 *m/z* and a resolution of 15,000. The exclusion time to reject masses from repetitive MS/MS fragmentation was set to 30 s.

Data analysis

The acquired MS spectra were processed in Proteome Discoverer (v1.4 and v2.1, Thermo Scientific). MS/MS spectra were searched against an *S. halorespirans* database containing 2,965 non-redundant protein-coding sequence entries (downloaded December 2016 from NCBI Genbank accession number CP017111.1) using the SEQUEST HT algorithm. Enzyme specificity was selected as trypsin with up to two missed cleavages allowed for the proteome-analysis and four missed cleavages allowed for the acetylome-analysis. The latter yielded more acetylated peptide hits than applying two or three missed cleavages in the searches. Peptide ion tolerance was set to 10 ppm and MS/MS tolerance to 0.02 Da. Oxidation (methionine) was selected as a dynamic and carbamidomethylation (cysteine) as a static modification. A maximum of three equal and four dynamic modifications per peptide were allowed. Only peptides with a false discovery rate (FDR) < 0.01, calculated by Percolator, and XCorr > 2.1 were considered as identified. Quantification of proteins was performed using the average of top three peptide MS1-areas. Protein quantification was considered successful for proteins quantified in > 50% of biological replicates, otherwise, they were classified as identified proteins. After log10 transformation, the protein values were median-normalized and scaled, so that the global minimum is zero. Throughout the text protein abundances are given in relation to the median of all proteins of a condition, i.e. > M+2σ relates to proteins with a higher abundance value than the median plus two standard deviations. MS1-areas of acetylated peptides which only differ in their modification status (oxidation, carbamidomethylation) were summed and counted as one acetylation site. To correct acetylation differences for different protein amounts, acetylation abundance ratios were obtained by subtracting the log-area of the most abundant acetylated peptide of a protein which was detected in at least two replicates from the logarithmized protein abundance values. For statistical analysis, data of proteins quantifiable in ≥ 50% of replicates were imputed using Prostar (imp4p, 10 iterations, no Lapala, http://www.prostar-proteomics.org). Differential proteome analysis was performed using a

211 Limma moderated t-test, corrected with the Benjamini – Hochberg method at false discovery rate
212 (FDR) < 0.05. P-values in the non-parametrical multiple dimensional scaling (nMDS)-plots were
213 calculated with the anosim-function of the vegan package in R v. 3.4.1 [20, 21]. The mass
214 spectrometry proteomics data have been deposited to the ProteomeXchange Consortium via the
215 PRIDE (https://www.ebi.ac.uk/pride) partner repository with the dataset identifier PXD008953.

216 Orthologs with *S. multivorans* and *E. coli* were obtained by using BLAST reciprocal best hits on the
217 Galaxy-platform (Minimum percentage identity 60% for *S. m.* and 35% for *E. c.*, Minimum percentage
218 query coverage 50%) [22, 23]. Data from Goris et al. [24] were re-analyzed using the same stringent
219 criteria to ensure comparability. Areas of the membrane and cytoplasm fraction were median-
220 transformed and summed. Protein localizations were calculated based on the amino acid sequence
221 using psortb version 3.0.2 [25]. Protein functions were determined with Prophane [26]. Enrichment
222 analyses were conducted using R packages clusterProfiler, dose and splitstackshape [27-29]. Figures
223 were created using R packages ggplot2, vegan and pheatmap [30, 31].

Results and Discussion

Long-term downregulation of PCE respiration in *Sulfurospirillum halorespirans*

In order to assess whether *S. halorespirans* shows the same kind of long-term downregulation of *pceA* gene expression as *S. multivorans* [2, 7], *S. halorespirans* was cultivated for 60 transfers with nitrate as sole electron acceptor (Fig. 1). This corresponds to approximately 200 generations. The amount and specific enzyme activity of PceA in crude extract decreased to about 1% of the initial activity detected in the presence of PCE (Fig. 2A, B), similar to the values observed for *S. multivorans* with fumarate or nitrate as electron acceptor [2, 7].

We extracted the proteome of *S. halorespirans* cultivated with tetrachloroethene (PCE) as electron acceptor (t0), and from cells that were cultivated for six (t6, short-term) or 60 transfers (t60 long-term cultivated) with nitrate as electron acceptor. Cells were harvested at the early and late exponential phase (Fig. S1). Of the in total 18 samples (six conditions, three replicates), 2,029 proteins could be identified (68% of the predicted proteome) and 1,799 proteins were quantifiable (i.e., had an abundance value in > 50% of all replicates). This was a substantial improvement compared to a previous study on *S. multivorans* cultivated with different electron donors and acceptors [7], where 1,716 proteins (53% coverage) were identified in 36 samples with less stringent filter criteria applied during proteome analysis. Of all identified proteins, 19% were predicted to be membrane-integral, according to classification by the localization prediction tool PSORTb [25] (Fig. S2A). This is closer to the theoretical value of 26% membrane-integral proteins than the 10% membrane-integral proteins identified in the study on *S. multivorans*. The distribution of protein sequence lengths of the measured proteome was almost identical to that of the predicted proteome, except for the underrepresented extremely small proteins of below 50 amino acids length (Fig. S2B). The bias against small proteins, however, was less than in the study on *S. multivorans*. This higher yield in protein identifications can be attributed to an optimized extraction protocol using harsher conditions with concentrated urea buffer and the combined use of trypsin and lysyl endopeptidase for a more efficient proteolytic cleavage [32] as opposed to *S. multivorans*, where a mild detergent (digitonin) was used. Consequently, our proteome dataset most likely represents the actual protein content of the cell closer than the previous study with *S. multivorans*.

Proteome dynamics during long-term cultivation without PCE

The number of identified proteins in samples gained from the three different subcultivation steps was similar (Fig. 3A). An nMDS was performed to assess the dissimilarity between protein abundances of the different time points. The results show a clear separation between the proteomes of t0, t6 and t60 cells, indicated by the reasonable variance and good reproducibility (Fig. 3C).

Further, we compared the protein functions under the different growth conditions. In PCE-grown cells, proteins of coenzyme metabolism, cell motility, and amino acid metabolism were significantly more abundant than in nitrate-grown cells (Fig. 4A). The significantly upregulated functional classes in t6 and t60 were similar to each other. These proteins were particularly related to translation and energy conservation. In t60, also proteins of the categories cell motility and amino acid metabolism were enriched compared to t6 cells.

OHR gene region

Analogous to the situation in the *S. multivorans* proteome [7], the most striking difference between cells adapted to PCE and to nitrate was the expression of the genes of the OHR core region. Among the overall five highest expressed proteins on PCE was the reductive dehalogenase PceA (> M+2σ, Tab. S1, S2, Fig. 5). It was among the 20 most differentially expressed proteins in PCE-grown cells compared to nitrate-grown cells (Tab. S3A), with downregulation in t6 to 11% of its original abundance and no quantifiable enzyme in t60. This is comparable to *S. multivorans*, where PceA had 0.1% of its original abundance in t60. Accordingly, its putative membrane anchor PceB was among the 20 most differentially produced proteins in t0 cells (Tab. S3B). Also, many other proteins encoded in the OHR gene region were among the most differentially produced proteins (Tab. S2, S3). Of all analyzed transfers, almost all quantifiable proteins encoded in the OHR region were highest abundant in t0 cells and were only slightly lower abundant in t6 (on average 57% of the abundance in t0). In t60, they were not detectable or only identifiable (Fig. 6B). Thus, most proteins showed a similar downregulation as the reductive dehalogenase PceA, including the putative quinol dehydrogenase (Qdh) and the norpseudo-B_{12} biosynthesis genes, suggesting the genes of the OHR region to be included within a single regulon.

279 Almost all proteins encoded in the OHR gene region were quantifiable after cultivation on PCE (Fig.
280 6B). This includes also several membrane-integral proteins, of which only a few were detected in the
281 *S. multivorans* dataset [5]. For example, the membrane subunit of the Qdh (SHALO_1506) was
282 detected in *S. halorespirans* t0 and t6 samples, underpinning its suggested role in the electron
283 transport chain (Fig. 5). Not quantifiable in both organisms were TCS I (SHALO_1498-1499) and the
284 second reductive dehalogenase RdhAB (SHALO_1500-1501), even though they are part of the 100%
285 conserved region in organohalide-respiring *Sulfurospirillum* spp. In both species, of RdhA, only one
286 peptide was identified in a single replicate and no *rdhA*-transcription could be detected in *S.*
287 *multivorans* [6, 7]. Other non- or only partly detected proteins may have escaped from extraction due
288 to their tight membrane interaction and/or small size, and include a small, putative membrane protein
289 possibly involved in electron transport (SHALO_1504), adenosylcobinamide-phosphate synthase CbiB
290 (SHALO_1507), the permease component BtuC of the corrinoid ABC transporter (SHALO_1516) and
291 the cysteine-rich SHALO_1512 and SHALO_1531 gene products.

292 Some proteins of the OHR core region were found in the proteomes of all conditions. Among them
293 was the TCS II response regulator (RR, SHALO_1503), with abundances between the median and
294 M+2δ of all proteins, and only found in 1.2-1.9-fold higher abundances in t0 cells (Fig. 5, 6B). The
295 corresponding histidine protein kinase (HK, SHALO_1502) was only quantifiable in the t0 and t6
296 proteomes. However, low amounts of this protein could have been undetected due to its seven
297 predicted transmembrane helices. Comparably to *S. multivorans*, only the TCS proteins encoded
298 adjacent to *rdhAB* rather than the one adjacent to *pceAB* were produced and therefore are most likely
299 involved in the regulation of OHR (Fig. 6B).

300 Nearly all proteins encoded by genes of the *cbi* cluster were detected in the proteome of *S.*
301 *halorespirans* (Fig. 6B, S3). These included several proteins which have not been assigned a function
302 and which were not quantifiable in *S. multivorans* [7], namely two cysteine-rich proteins
303 (SHALO_1512, SHALO_1531) and the MsbA-like protein (SHALO_1529). The cysteine-rich proteins
304 could play a role in metal supply or unknown redox processes in corrinoid biosynthesis. The MsbA-like
305 putative lipid A export protein is probably not involved in the transport of corrinoids or cobalt, as these
306 roles are already assigned to BtuCDF (SHALO_1516-1518) and the ECF cobalt transporter
307 (SHALO_1589-1593), respectively. Both of these transporters were quantified in the proteomes of
308 both species (Fig. S3, Tab. S1) [7]. Aside from similarities of the SHALO_1529 gene product to MsbA

309 (30% amino acid sequence similarity), which might suggest a role in lipid export, nothing is currently
310 known about its function.

311 One of the observed differences between the *S. multivorans* and *S. halorespirans* OHR gene region
312 was the presence of 106 inserted nucleotides upstream of the *cbi* gene cluster in the latter [6]. A
313 putative ORF is located in this region, but no peptides were detected when the proteome data were
314 searched against a 6-frame-translation-database. It either escaped proteomic detection due to its
315 small size or the region does not encode an ORF but serves regulatory functions. Downstream of the
316 *cbi* gene region, a regulatory gene encodes a TetR-like transcriptional repressor, which could not be
317 assigned a function up to now. The TetR-like transcriptional regulator (SHALO_1533) was produced to
318 low abundances (< M-1σ) on PCE. The abundance of the proteins encoded downstream of the
319 corresponding gene, however, showed a similar pattern as in *S. multivorans* (Fig. 6B): Two flavin-
320 containing proteins (SHALO_1534, SHALO_1536) were among the most abundant proteins in the
321 proteome of PCE-cultivated cells (Tab. S2) and have an abundance level similar to PceA. However,
322 both were also detectable in the proteome in t60. Based on its sequence, SHALO_1534 is predicted to
323 be an electron-transfer flavoprotein, whereas SHALO_1536 is classified to a group of redox proteins,
324 which also includes pyridoxamine 5'-phosphate oxidases involved in the vitamin B_6 metabolism. They
325 were suggested to play a role in corrinoid biosynthesis or modification [7], but their presence even
326 after 60 transfers without PCE remains enigmatic.

327 The proteins encoded in the regions flanking the OHR core region (SHALO_1480-1493,
328 SHALO_1538-1554, Fig. 6A) are hardly detectable in any of the proteomes of *S. halorespirans* or *S.*
329 *multivorans* (Tab. S1) [7] and their role remains obscure. The contained genes are conserved in the
330 two organohalide-respiring species *S. multivorans* and *S. halorespirans* and do not have orthologs in
331 the *S. deleyianum* and *S. barnesii*, which are not capable of OHR [6, 8]. Only a hypothetical protein
332 (SHALO_1552) and a putative membrane-bound protein (SHALO_1553) were detected but showed
333 low abundance levels (< M). To conclude, production of almost all proteins encoded in the OHR core
334 region continues during the absence of PCE and only ceases after prolonged cultivation without their
335 specific substrate in *S. halorespirans*, comparable to *S. multivorans*, suggesting that the three
336 differences in the OHR region have no detectable influence on the long-term downregulation.

PCE-induced proteins outside the OHR gene region

The outer membrane porin SHALO_0946 was among the 20 most abundant proteins in t0 (Tab. S2), whereas on nitrate, it only had a rank ranging from 187 to 310, and was significantly more abundant in t0 than in t6 (Tab. S1), indicating a role in PCE-import. The only stress-related protein among the 20 most differentially produced proteins was the heat shock protein Hsp20 (SHALO_0540), which was up to 12-fold higher on PCE (Tab. S3). The biosynthesis of this protein was also found to be PCE-dependent in *S. multivorans* [7]. The higher abundance of Hsp20 in both proteomes strengthens our suggestion for its role in a PCE-dependent stress response.

Proteins involved in nitrate respiration

Proteins related to nitrate respiration were among the most abundant proteins in *S. halorespirans* cells cultivated with nitrate (Tab. S2). In general, coverage of proteins involved in nitrate respiration was higher than in *S. multivorans*: All subunits of the nitrate reductase NapAGHBLD (SHALO_0949-0955) and the nitrite reductase NrfHAIJ (SHALO_0905-0908) were quantified with abundances of up to > M+2σ (Fig. S4, Tab. S1). Most of the Nos proteins, responsible for the reduction of nitrous oxide to nitrogen (encoded by SHALO_0349-0357), were produced in *S. halorespirans* to abundances below median under all conditions but higher with nitrate than with PCE. For unknown reasons, NosZ (SHALO_0357) was only detected in PCE-grown cells. In *S. multivorans*, this cluster is not encoded [8]. As in *S. multivorans*, on nitrate, the hydroxylamine reductase (SHALO_0596) had similar abundances as Nap and Nrf, but it was also quantifiable on PCE. It was suggested to scavenge intermediates formed during denitrification, such as nitrite or nitric oxide [7]. An outer membrane porin (SHALO_2097) was up to 44-fold higher abundant on nitrate (Tab. S3A), indicating a specific function in nitrate import.

Other redox proteins involved in the energy metabolism

In the proteome of *S. halorespirans*, two proteins were quantified serving the oxidation of the electron donor pyruvate, the pyruvate:ferredoxin/flavodoxin oxidoreductase (PFOR, SHALO_2324) and the quinone-dependent pyruvate dehydrogenase (PoxB, SHALO_1660, exclusively identified in organohalide-respiring *Sulfurospirillum* spp. up to now [7]). Opposed to *S. multivorans*, PoxB might

have lower importance in *S. halorespirans*, since the abundance of this enzyme was up to 800-fold less than that of PFOR (Tab. S1).

Ferredoxin most probably serves in accepting the electrons from pyruvate oxidation via PFOR (Fig. 5). Similar to *S. multivorans*, ferredoxin SHALO_0269 (ortholog SMUL_0303) was produced, even though lower abundant in *S. halorespirans* (around median vs. > M+σ). Additionally and opposed to *S. multivorans*, two other ferredoxins were quantifiable, SHALO_0929 (SMUL_0908) and, preferentially in the late exponential phase, SHALO_0278 (SMUL_0312). These ferredoxins are conserved in most Epsilonproteobacteria [6]. Furthermore, ferredoxin SHALO_1216 (SMUL_1235), which is encoded in the nitrogenase gene region, was quantified, whereas the nitrogenase itself was not found. As in *S. multivorans*, flavodoxins (SHALO_1212, SHALO_2554) were not detected, stressing the role of ferredoxin as a central electron carrier in *Sulfurospirillum* spp.

As in *S. multivorans*, of the four encoded hydrogenases, the periplasmic membrane-bound NiFe hydrogenase (MBH, SHALO_1400-1402) was constitutively produced to high abundances under all conditions (up to > M+2σ), even though the cultures were not supplied with hydrogen. Interestingly, the putative hydrogen-evolving Ech-like hydrogenase Coo (SHALO_1293-1297) did show a PCE-dependent production. This hydrogenase has never been detected in *S. multivorans* [7]. The hydrogenase-4 Hyf (SHALO_2129-2141) bears a frameshift mutation caused by a transposon insertion, which is the reason why only few of its subunits were produced, in contrast to *S. multivorans*. This presumably also explains the observation that *S. halorespirans* cannot be cultivated on pyruvate alone, in contrast to *S. multivorans*, which can grow fermentatively on pyruvate without any electron acceptor [33]. Hyf might also function as an electron sink using the electrons from ferredoxin to generate H_2 when excess electron donor is supplied. Coo might partly substitute the defective Hyf in *S. halorespirans*.

Apart from the small differences in the genome, some physiological differences to *S. multivorans* became apparent, among them the more important role of chemotaxis in *S. halorespirans*. Among the proteins encoded in both species but produced to a much higher level in *S. halorespirans*, were 20 chemotaxis proteins. Most of the chemotaxis-related proteins had abundances of at least M+σ (Tab. S1) and were up to 400-times higher in *S. halorespirans* or not even produced in *S. multivorans* (Tab.

S4). Similar to *S. multivorans* [7], cell motility-related proteins were enriched within the significantly more abundant proteins of t0- compared to t60-cells (Fig. 4A).

Acetylome

Protein acetylations are more and more recognized as an important modifier of protein activity and function. This comprehensive lysine-acetylome study was designed in order to prove the hypothesis that acetylations of key regulators are involved in controlling long-term regulation in *S. halorespirans*. This first acetylome of an Epsilonproteobacterium revealed that one-third of all identified proteins possess acetylation sites (Fig. 3B). This corresponds to 22% of the predicted proteome in *S. halorespirans* (Tab. S5) and is a relatively large number compared to on average 9% acetylated proteins in comparable studies of other bacteria [34], implying that acetylations are involved in many physiological processes in *S. halorespirans*. Of the 640 identified acetylated proteins, 368 were acetylated at various Lys sites (57%, Fig. 3B). Proteins with the most acetylation sites were PFOR (SHALO_2324, 29 sites, highest in t6), heat shock protein 60 family chaperone GroEL (SHALO_1004), chaperone protein DnaK (SHALO_1713) and ferredoxin-sulfite reductase (SHALO_2857, 22 sites each and highest in t6, Tab. S1). Apart from the latter, these highly acetylated proteins had also acetylated orthologs in *E. coli* and are in general known to be targets for lysine acetylations (e.g. [35-37]), even though their exact role is unknown, as in general, to date, only little has been explored about specific effects of protein acetylations.

60% of the acetylated proteins in *S. halorespirans* had orthologs in *E. coli* and 58% of these orthologs were also acetylated in *E. coli*. This and the constitutive production of most of these proteins under all conditions points at a higher incidence of acetylations on housekeeping proteins (Tab. S1). Furthermore, the more acetylation sites on a protein, the higher was the conversation grade of the protein in *E. coli* and its probability to be acetylated as well, i.e. to be found in the CPLM database of lysine-modified proteins (Fig. S5). The enrichment of acetylated proteins in energy conservation, translation and nucleotide metabolism (Fig. 4B) is consistent with previous studies of other bacteria [34, 38], indicating the conserved role of acetylations in the regulation of physiological processes.

The nMDS analysis of the acetylome resulted in a significant segregation of t0, t6 and t60 samples ($p = 0.001$), indicating that the acetylation pattern differed between transfers (Fig. 3D). Most acetylated proteins were detected in t6 (EL t0 vs. t6 $p = 0.0005$, EL t6 vs. t60 $p = 0.002$, Fig. 3A), which might

421 reflect the metabolic transition of *S. halorespirans* adapting to a different electron acceptor. Only one
422 acetyltransferase was higher abundant in t6 than in other phases, namely a putative N-
423 acetyltransferase (SHALO_1415).

424 Two flavoproteins (SHALO_1534 and SHALO_1536) encoded in the OHR gene region were
425 acetylated (Fig. 6C, D). There are several studies about flavoproteins which are inhibited by
426 acetylations, e.g. the flavoprotein subunit of the succinate dehydrogenase [35, 39] and the pyridoxine
427 5'-phosphate oxidase [40-42].

428 **Acetylation of the two-component system**

429 In TCS II (SHALO_1502-1503), which is most probably involved in the regulation of PCE respiration
430 [6, 7], several acetylated sites were identified and their spectra manually curated (Fig. S6). The
431 number of acetylations in the TCS II was at a maximum in the transition phase (t6), when the OHR
432 genes were expressed in the absence of PCE (Tab. S6). The HK (SHALO_1502) was acetylated in
433 two out of three replicates of the sample harvested in the late exponential phase and in one of three
434 replicates in the early exponential phase of t6. In t0, no HK acetylations were detected and in t60, the
435 HK was not identified in the proteome. The acetylated K598 is part of the catalytic domain, which
436 belongs to the HATPase_c domain family, and is located adjacent to the ATP-binding site. The
437 acetylated lysine clashes with the amino acids D552 and S553 in the structural model of the HK (Fig.
438 7A, B). However, the mode of influencing the protein functionality might be indirect, since the K598
439 side chain is most likely oriented outwards the protein with some steric freedom.

440 The cognate response regulator shows two acetylations in t6, K114 and K218, of which only K114 was
441 detected in t0 but with lower abundance (Tab. S6). Acetylation of K114 during t60 was only present in
442 one replicate (of EE and EL), interestingly the one, in which PceA was also identified (Tab. S1). The
443 acetylation of K114 was highly abundant (> M+σ) and found in three replicates of the early and in two
444 replicates of the late exponential phase of t6 (Fig. 6D). In the predicted structural model of the RR, an
445 acetylation of K114, which is part of the receiver domain (REC), would interfere with D111 of the REC
446 domain (Fig. 8A, B). The acetylation of K218 was detected in only one replicate of the early
447 exponential phase of t6. K218 is located at the C-terminus of the DNA binding domain and part of the
448 smaller β-sheet. In the structural model, the acetylation is exposed to the protein surface and
449 interferes most likely with N171 (Fig. 8C), which is likewise part of the DNA-binding domain. Both

amino acids face away from the DNA and both acetylation sites are most probably not directly involved in intramolecular interactions. Although no direct effect of the acetylations can be concluded, the specificity and stability of protein-protein interactions or protein-DNA binding as well as the efficiency of the initiation of the transcription could be influenced by conformational changes or neutralization of the positive charge of a lysine.

Overall, the acetylations specific for t6 during the transition phase could have both, an activating or an inhibiting effect on the gene regulation of the OHR gene cluster. Assuming that the phosphorylation of the RR by the HK has stopped, acetylation might mimic the phosphorylation and keep the RR in the active, DNA-binding state but with lower affinity (Fig. 5). An activating effect was described for the transcription factor HilD in *Salmonella enterica* serovar Typhimurium, which is stabilized by an acetylation leading to a continuous gene expression [43]. However, of the few TCSs analyzed for their functional modulation by acetylation, mainly inhibiting effects have been reported. An acetylation within the winged HTH motif was described to decrease the DNA-binding activity of the RR RcsB in *E. coli* [44, 45] and PhoP in *S. enterica* serovar Typhimurium [46] but only slightly of the global RR GlnR in *Streptomyces coelicolor* [47]. Another RR, CheY, regulating chemotaxis in *E. coli*, was described to have a repressed binding affinity to all target proteins due to lysine acetylation [48, 49]. *In vivo,* two acetylation sites of CheY are located within the receiver domain and one within the active site, which is part of the dimerization interface [49]. In general, the acetylation of the TCS II in *S. halorespirans* could lead to a reduction in the protein stability, the dimerization of the RR or its promoter binding affinity. Assuming that the phosphorylation of the RR by the HK is not immediately ceasing in the absence of PCE, this loss in functionality of the RR might cause the delay in OHR gene expression.

Other RRs were suggested to be specifically acetylated via an N-acetyltransferase [44-49] and deacetylated via a Sir2 family deacetylase [44, 46, 47, 49]. In *Sulfurospirillum* spp. the putative N-acetyltransferase (SHALO_1415), which was higher abundant in t6 than at other time points (Fig. 5), and the NAD^+-dependent protein deacetylase of the Sir2 family (SHALO_1877), which is the only annotated Sir2 family deacetylase in the genome of *S. halorespirans*, might be responsible for the acetylation and deacetylation of the TCS II. The characterization of the molecular mechanism of the signal transduction via phosphorylation and further fine-tuning via acetylation as well as its impact on the maintenance of the gene expression of the OHR gene cluster in the absence of PCE should be investigated in future studies.

Conclusion

In this study, we proved that tetrachloroethene respiration of *Sulfurospirillum halorespirans* is long-term regulated. The physiology of PCE respiration seems to be similar to *S. multivorans*, although some differences were observed in the pyruvate-oxidizing enzymes and the ferredoxin abundance. The regulation of OHR in *Sulfurospirillum* spp. seems to depend mainly on a two-component regulatory system. The acetylome provided evidence that acetylations might play a major role in the OHR gene expression regulation via the TCS II. However, our findings need to be confirmed by *in vitro* studies with the regulatory gene products.

Acknowledgement

This work was supported by the German Research Foundation (DFG), as part of the research group FOR 1530. D.T. was also supported by the Helmholtz Interdisciplinary Graduate School for Environmental Research (HIGRADE). J.E. was supported by the International Leibniz Research School (ILRS).

References

[1] L.A. Hug, F. Maphosa, D. Leys, F.E. Löffler, H. Smidt, E.A. Edwards, L. Adrian, Overview of organohalide-respiring bacteria and a proposal for a classification system for reductive dehalogenases, Philo Trans R Soc Lond B Biol Sci 368(1616) (2013).

[2] M. John, R. Rubick, R.P. Schmitz, J. Rakoczy, T. Schubert, G. Diekert, Retentive memory of bacteria: Long-term regulation of dehalorespiration in *Sulfurospirillum multivorans*., J. Bacteriol. 191(5) (2009) 1650-5.

[3] A. Duret, C. Holliger, J. Maillard, The Physiological Opportunism of *Desulfitobacterium hafniense* Strain TCE1 towards Organohalide Respiration with Tetrachloroethene, Appl. Environ. Microbiol. 78(17) (2012) 6121-6127.

[4] T. Goris, B. Hornung, T. Kruse, A. Reinhold, M. Westermann, P.J. Schaap, H. Smidt, G. Diekert, Draft genome sequence and characterization of *Desulfitobacterium hafniense* PCE-S, Stand Genomic Sci 10 (2015) 15-15.

[5] T. Futagami, Y. Tsuboi, A. Suyama, M. Goto, K. Furukawa, Emergence of two types of nondechlorinating variants in the tetrachloroethene-halorespiring *Desulfitobacterium* sp. strain Y51, Appl. Microbiol. Biotechnol. 70(6) (2006) 720-728.

[6] T. Goris, T. Schubert, J. Gadkari, T. Wubet, M. Tarkka, F. Buscot, L. Adrian, G. Diekert, Insights into organohalide respiration and the versatile catabolism of *Sulfurospirillum multivorans* gained from comparative genomics and physiological studies, Environ. Microbiol. 16(11) (2014) 3562-80.

[7] T. Goris, C.L. Schiffmann, J. Gadkari, T. Schubert, J. Seifert, N. Jehmlich, M. von Bergen, G. Diekert, Proteomics of the organohalide-respiring Epsilonproteobacterium *Sulfurospirillum multivorans* adapted to tetrachloroethene and other energy substrates, Sci. Rep. 5 (2015) 13794.

[8] T. Goris, B. Schenz, J. Zimmermann, M. Lemos, J. Hackermüller, T. Schubert, G. Diekert, The complete genome of the tetrachloroethene-respiring Epsilonproteobacterium *Sulfurospirillum halorespirans*, J. Biotechnol. (2017).
[9] G.F. Buttet, A.M. Murray, T. Goris, M. Burion, B. Jin, M. Rolle, C. Holliger, J. Maillard, Coexistence of two distinct *Sulfurospirillum* populations respiring tetrachloroethene – genomic and kinetic considerations, FEMS Microbiol. Ecol. (2018) fiy018-fiy018.
[10] V.J. Carabetta, I.M. Cristea, Regulation, Function, and Detection of Protein Acetylation in Bacteria, J. Bacteriol. 199(16) (2017) 3713-3721.
[11] H. Scholz-Muramatsu, A. Neumann, M. Messmer, E. Moore, G. Diekert, Isolation and characterization of *Dehalospirillum multivorans* gen. nov., sp. nov., a tetrachloroethene-utilizing, strictly anaerobic bacterium, Arch Microbiol 163(1) (1995) 48-56.
[12] A. Neumann, G. Wohlfarth, G. Diekert, Purification and characterization of tetrachloroethene reductive dehalogenase from *Dehalospirillum multivorans*, J. Biol. Chem. 271(28) (1996) 16515-9.
[13] Y. Zhang, I-TASSER server for protein 3D structure prediction, BMC Bioinformatics 9(1) (2008) 40.
[14] A. Roy, A. Kucukural, Y. Zhang, I-TASSER: a unified platform for automated protein structure and function prediction, Nat. Protoc. 5(4) (2010) 725-738.
[15] M.J. Bick, V. Lamour, K.R. Rajashankar, Y. Gordiyenko, C.V. Robinson, S.A. Darst, How to Switch Off a Histidine Kinase: Crystal Structure of *Geobacillus stearothermophilus* KinB with the inhibitor Sda, J. Mol. Biol. 386(1) (2009) 163-177.
[16] N. Friedland, T.R. Mack, M. Yu, L.-W. Hung, T.C. Terwilliger, G.S. Waldo, A.M. Stock, Domain Orientation in the Inactive Response Regulator *Mycobacterium tuberculosis* MtrA Provides a Barrier to Activation, Biochemistry 46(23) (2007) 6733-6743.
[17] A. Warnecke, T. Sandalova, A. Achour, R.A. Harris, PyTMs: a useful PyMOL plugin for modeling common post-translational modifications, BMC Bioinformatics 15(1) (2014) 370.
[18] L. Schrodinger, The PYMOL Molecular Graphics System, Version 1.1.4.4, 2010.
[19] A. Guo, H. Gu, J. Zhou, D. Mulhern, Y. Wang, K.A. Lee, V. Yang, M. Aguiar, J. Kornhauser, X. Jia, J. Ren, S.A. Beausoleil, J.C. Silva, V. Vemulapalli, M.T. Bedford, M.J. Comb, Immunoaffinity Enrichment and Mass Spectrometry Analysis of Protein Methylation, Mol. Cell. Proteomics 13(1) (2014) 372-387.
[20] F.G.B. Jari Oksanen, Michael Friendly, Roeland Kindt, Pierre Legendre, Dan McGlinn, Peter R. Minchin, R. B. O'Hara, Gavin L. Simpson, Peter Solymos, M. Henry H. Stevens, Eduard Szoecs and Helene Wagner, vegan: Community Ecology Package. R package version 2.4-5, 2017.
[21] R.C. Team, R: A Language and Environment for Statistical Computing. R Foundation for Statistical Computing, Vienna (2014). R Foundation for Statistical Computing, 2017.
[22] C. Camacho, G. Coulouris, V. Avagyan, N. Ma, J. Papadopoulos, K. Bealer, T.L. Madden, BLAST+: architecture and applications, BMC Bioinformatics 10(1) (2009) 421.
[23] P.J.A. Cock, J.M. Chilton, B. Grüning, J.E. Johnson, N. Soranzo, NCBI BLAST+ integrated into Galaxy, GigaScience 4(1) (2015) 1-7.
[24] T. Goris, C.L. Schiffmann, J. Gadkari, L. Adrian, M. von Bergen, G. Diekert, N. Jehmlich, Proteomic data set of the organohalide-respiring Epsilonproteobacterium *Sulfurospirillum multivorans* adapted to tetrachloroethene and other energy substrates, Data Brief 8 (2016) 637-642.
[25] N.Y. Yu, J.R. Wagner, M.R. Laird, G. Melli, S. Rey, R. Lo, P. Dao, S.C. Sahinalp, M. Ester, L.J. Foster, F.S.L. Brinkman, PSORTb 3.0: improved protein subcellular localization prediction with refined localization subcategories and predictive capabilities for all prokaryotes, Bioinformatics 26(13) (2010) 1608-1615.
[26] T. Schneider, E. Schmid, J.V. de Castro, M. Cardinale, L. Eberl, M. Grube, G. Berg, K. Riedel, Structure and function of the symbiosis partners of the lung lichen (*Lobaria pulmonaria* L. Hoffm.) analyzed by metaproteomics, Proteomics 11(13) (2011) 2752-2756.
[27] A. Mahto, splitstackshape: Stack and Reshape Datasets After Splitting Concatenated Values. R package version 1.4.2, 2014.
[28] G. Yu, L.-G. Wang, Y. Han, Q.-Y. He, clusterProfiler: an R Package for Comparing Biological Themes Among Gene Clusters, OMICS 16(5) (2012) 284-287.

[29] G. Yu, L.-G. Wang, G.-R. Yan, Q.-Y. He, DOSE: an R/Bioconductor package for disease ontology semantic and enrichment analysis, Bioinformatics 31(4) (2015) 608-609.
[30] R. Kolde, pheatmap: Pretty Heatmaps. R package version 1.0.8, 2015.
[31] H. Wickham, ggplot2: Elegant Graphics for Data Analysis Springer-Verlag, New York (2009).
[32] B.T. Weinert, S.A. Wagner, H. Horn, P. Henriksen, W.R. Liu, J.V. Olsen, L.J. Jensen, C. Choudhary, Proteome-Wide Mapping of the *Drosophila* Acetylome Demonstrates a High Degree of Conservation of Lysine Acetylation, Sci Signal 4(183) (2011) ra48-ra48.
[33] S. Kruse, T. Goris, M. Westermann, L. Adrian, G. Diekert, Hydrogen production by *Sulfurospirillum* spp. enables syntrophic interactions of Epsilonproteobacteria, bioRxiv (2017) doi: 10.1101/238212.
[34] T. Ouidir, T. Kentache, J. Hardouin, Protein lysine acetylation in bacteria: Current state of the art, Proteomics 16(2) (2016) 301-9.
[35] B.T. Weinert, V. Iesmantavicius, S.A. Wagner, C. Scholz, B. Gummesson, P. Beli, T. Nystrom, C. Choudhary, Acetyl-phosphate is a critical determinant of lysine acetylation in *E. coli*, Mol. Cell 51(2) (2013) 265-72.
[36] V.J. Carabetta, T.M. Greco, A.W. Tanner, I.M. Cristea, D. Dubnau, Temporal Regulation of the *Bacillus subtilis* Acetylome and Evidence for a Role of MreB Acetylation in Cell Wall Growth, mSystems 1(3) (2016) e00005-16.
[37] C.A. Butler, P.D. Veith, M.F. Nieto, S.G. Dashper, E.C. Reynolds, Lysine acetylation is a common post-translational modification of key metabolic pathway enzymes of the anaerobe *Porphyromonas gingivalis*, J Proteom 128(Supplement C) (2015) 352-364.
[38] J. Liu, Q. Wang, X. Jiang, H. Yang, D. Zhao, J. Han, Y. Luo, H. Xiang, Systematic Analysis of Lysine Acetylation in the Halophilic Archaeon *Haloferax mediterranei*, J. Proteome Res. 16(9) (2017) 3229-3241.
[39] H. Cimen, M.-J. Han, Y. Yang, Q. Tong, H. Koc, E.C. Koc, Regulation of Succinate Dehydrogenase Activity by SIRT3 in Mammalian Mitochondria, Biochemistry 49(2) (2010) 304-311.
[40] B. Schilling, D. Christensen, R. Davis, A.K. Sahu, L.I. Hu, A. Walker-Peddakotla, D.J. Sorensen, B. Zemaitaitis, B.W. Gibson, A.J. Wolfe, Protein acetylation dynamics in response to carbon overflow in *Escherichia coli*, Mol Microbiol 98(5) (2015) 847-863.
[41] L. Liu, G. Wang, L. Song, B. Lv, W. Liang, Acetylome analysis reveals the involvement of lysine acetylation in biosynthesis of antibiotics in *Bacillus amyloliquefaciens*, Sci Rep 6 (2016) 20108.
[42] J. Gu, Y. Chen, H. Guo, M. Sun, M. Yang, X. Wang, X. Zhang, J. Deng, Lysine acetylation regulates the activity of Escherichia coli pyridoxine 5'-phosphate oxidase, Acta Biochim Biophys Sin 49(2) (2017) 186-192.
[43] Y. Sang, J. Ren, J. Ni, J. Tao, J. Lu, Y.-F. Yao, Protein Acetylation Is Involved in *Salmonella enterica* Serovar Typhimurium Virulence, J. Infect. Dis. 213(11) (2016) 1836-1845.
[44] S. Thao, C.-S. Chen, H. Zhu, J.C. Escalante-Semerena, N^{ε}–Lysine Acetylation of a Bacterial Transcription Factor Inhibits Its DNA-Binding Activity, PLoS One 5(12) (2011) e15123.
[45] L.I. Hu, B.K. Chi, M.L. Kuhn, E.V. Filippova, A.J. Walker-Peddakotla, K. Bäsell, D. Becher, W.F. Anderson, H. Antelmann, A.J. Wolfe, Acetylation of the Response Regulator RcsB Controls Transcription from a Small RNA Promoter, J Bacteriol 195(18) (2013) 4174-4186.
[46] J. Ren, Y. Sang, Y. Tan, J. Tao, J. Ni, S. Liu, X. Fan, W. Zhao, J. Lu, W. Wu, Y.-F. Yao, Acetylation of Lysine 201 Inhibits the DNA-Binding Ability of PhoP to Regulate *Salmonella* Virulence, PLoS Pathog. 12(3) (2016) e1005458.
[47] R. Amin, M. Franz-Wachtel, Y. Tiffert, M. Heberer, M. Meky, Y. Ahmed, A. Matthews, S. Krysenko, M. Jakobi, M. Hinder, J. Moore, N. Okoniewski, B. Maček, W. Wohlleben, A. Bera, Post-translational Serine/Threonine Phosphorylation and Lysine Acetylation: A Novel Regulatory Aspect of the Global Nitrogen Response Regulator GlnR in *S. coelicolor* M145, Front. Mol. Biosci. 3(38) (2016).
[48] O. Liarzi, R. Barak, V. Bronner, M. Dines, Y. Sagi, A. Shainskaya, M. Eisenbach, Acetylation represses the binding of CheY to its target proteins, Mol. Microbiol. 76(4) (2010) 932-943.

[49] R. Li, J. Gu, Y.-Y. Chen, C.-L. Xiao, L.-W. Wang, Z.-P. Zhang, L.-J. Bi, H.-P. Wei, X.-D. Wang, J.-Y. Deng, X.-E. Zhang, CobB regulates *Escherichia coli* chemotaxis by deacetylating the response regulator CheY, Mol. Microbiol. 76(5) (2010) 1162-1174.

Figures

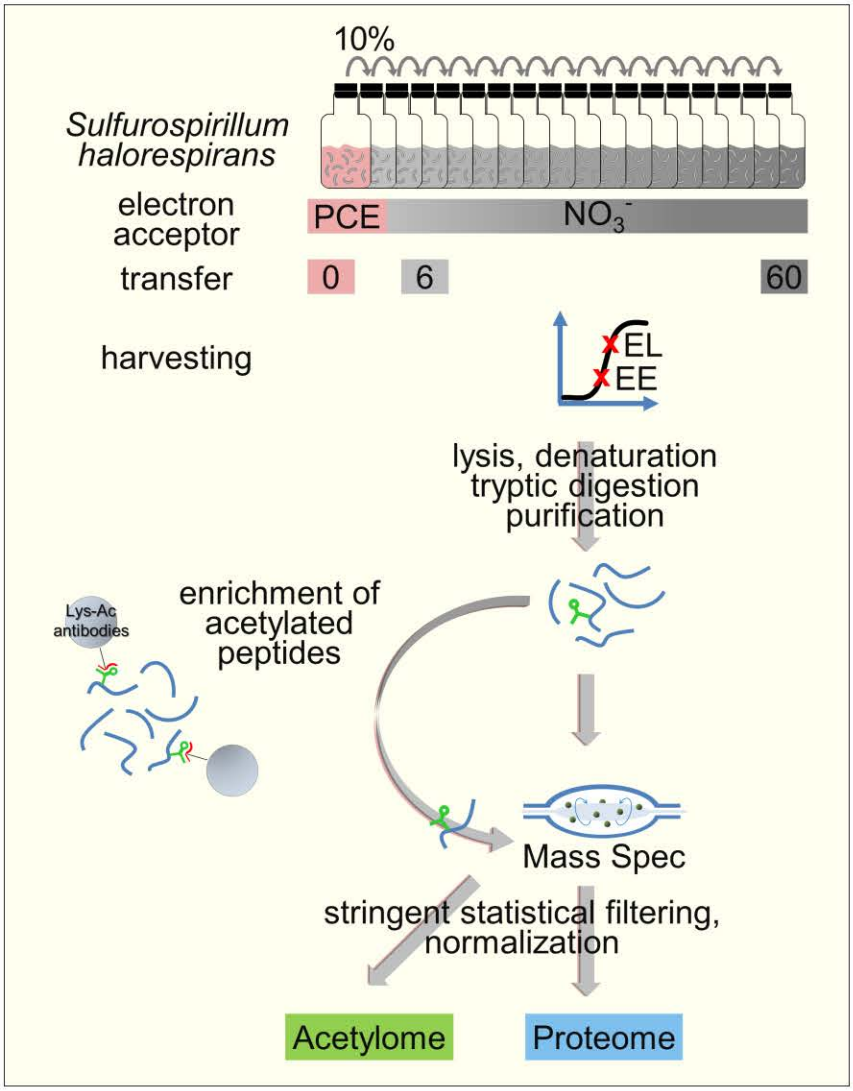

Fig. 1. Monitoring the proteomic and acetylation profile of *S. halorespirans* during cultivation on different electron acceptors. Three biological replicates of *S. halorespirans* were cultivated with PCE/pyruvate (t0, transfer 0) and subsequently on nitrate/pyruvate (t1-t60). Each culture was inoculated with 10 % of a culture in exponential phase. Protein was extracted and digested from t0, t6 and t60 during early (EE) or late exponential (EL) growth phase. A subfraction of the peptide digest was subjected to acetylpeptide enrichment. Peptide and acetylpeptide digest were analyzed by LC-MS/MS, followed by bioinformatic analysis.

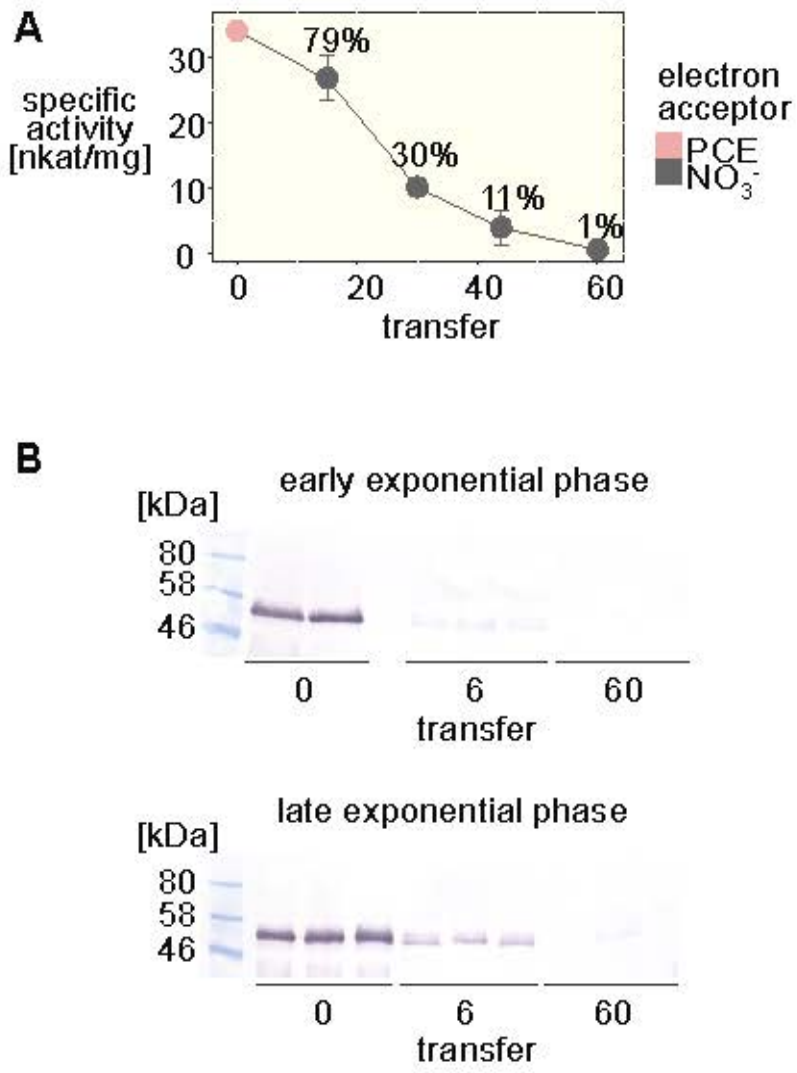

628

629 Fig. 2. (A) PCE dechlorination activity of PceA in crude cell extracts from *S. halorespirans*.
630 Photometrically measured with reduced methyl viologen as electron donor. Activity presented from
631 cells cultivated with PCE (t0, 100% activity) and from cells cultivated for 15, 30, 44 and 60 successive
632 transfers to medium with nitrate as sole electron acceptor. (B) Immunostaining of PceA in crude
633 extracts from *S. halorespirans* cultivated with PCE (t0) or for six or 60 transfers with nitrate (t6, t60). 10
634 µg protein per lane applied to SDS-PAGE, subsequent blotting to a PVDF membrane. Biological
635 replicates of the samples harvested after the transfers t0, t6 and t60 during the early (OD_{578} ≈ 0.11)
636 and late exponential (OD_{578} ≈ 0.20) growth phase are shown.

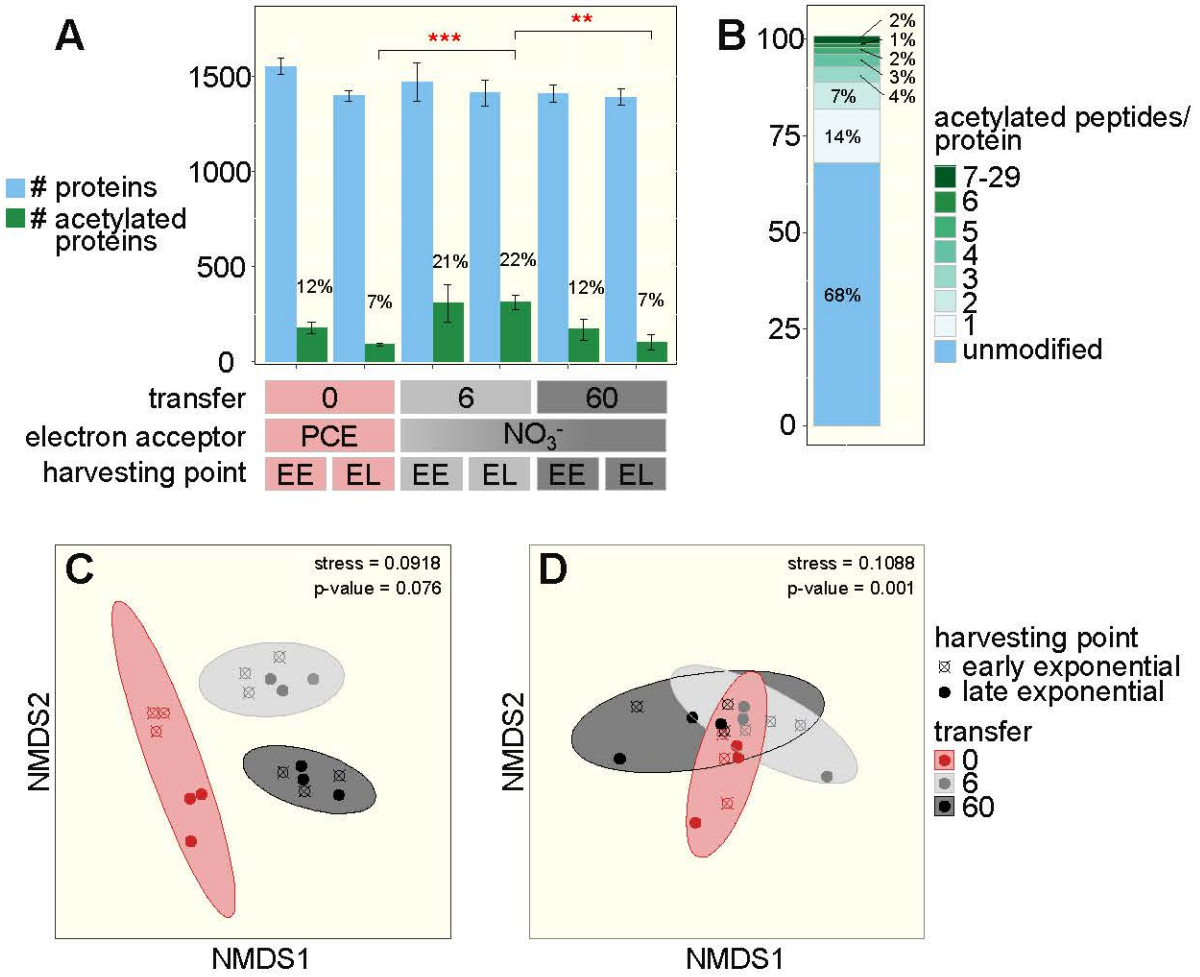

637

638 Fig. 3. (A) Number of quantifiable proteins and proteins with at least one acetylation site and p-values
639 of differences between transfers if significant: **, $p < 0.01$; ***, $p < 0.001$. (B) Number of acetylation
640 sites per protein (C) nMDS-analysis of proteome profiles (D) nMDS-analysis of acetylome profiles
641 (logarithmized average of top three acetylated peptide areas normalized to the intensity of the
642 corresponding unmodified protein).

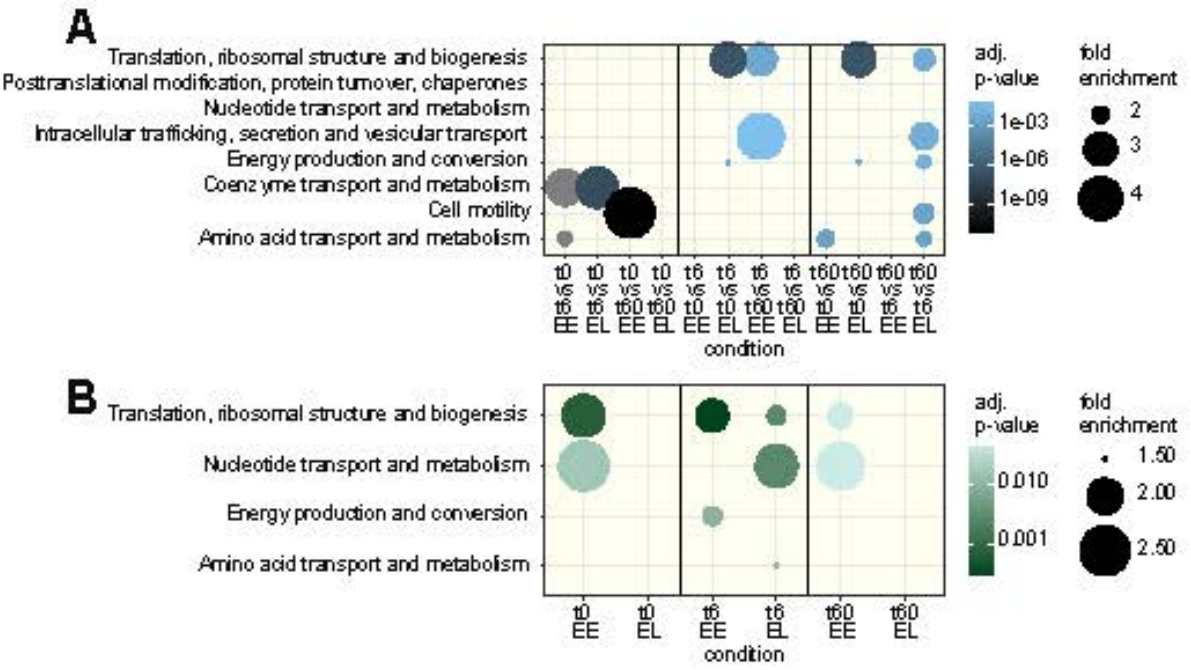

643

644 Fig. 4. Enrichment analysis of functional protein classes. (A) Functional protein classes
645 overrepresented within the significantly upregulated proteins ($p < 0.05$) of cells cultivated on PCE (t0)
646 compared to cells cultivated for six or 60 transfers on nitrate (t6, t60). (B) Functional protein classes
647 overrepresented within the acetylated proteins compared to all proteins of each condition. Y-axis lists
648 the COG-subrole terms, x-axis the compared conditions, bubble size corresponds to fold enrichment
649 of the respective pathway among the significantly regulated proteins in the condition mentioned first,
650 color scale and values adjacent to bubbles correspond to the adjusted p-values. EE, early exponential
651 phase; EL, late exponential phase.

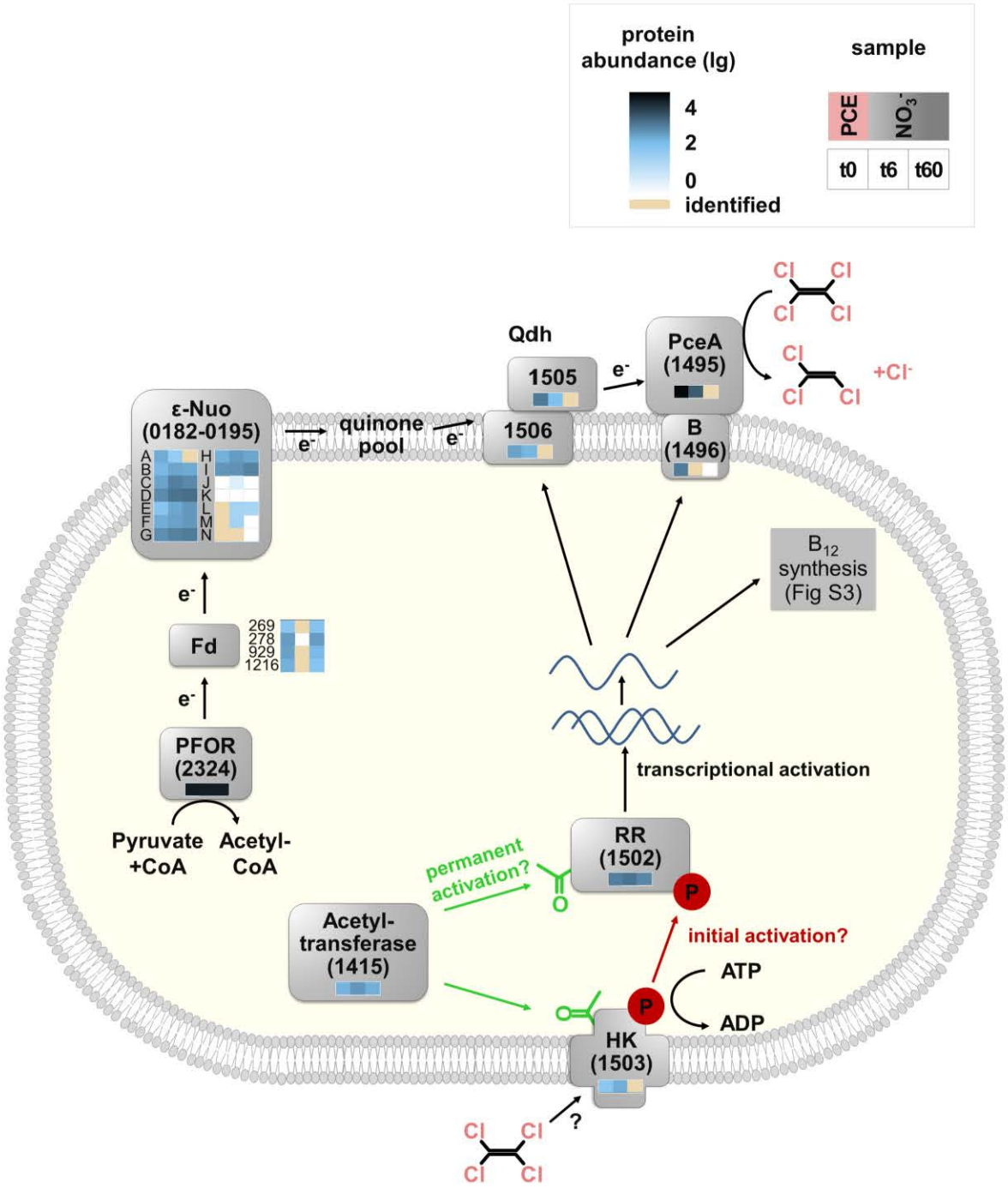

652

653 Fig. 5. Model of the organohalide respiratory chain and its putative two-component regulatory system
654 in *S. halorespirans* with pyruvate as electron donor. The locus tag suffix (prefix SHALO) and the
655 average protein abundances with PCE (t0), after six (t6) and 60 transfers (t60) with nitrate are given
656 as heat maps inside the protein sketches. PCE is reduced with electrons derived from pyruvate
657 oxidation, the route of electrons is indicated with arrows. PCE is probably sensed by the histidine
658 kinase, which is autophosphorylated and transfers the signal by phosphorylating the response

659 regulator. The phosphorylated response regulator binds the DNA, which leads to expression of the
660 OHR gene region. The acetyltransferase SHALO_1415 is a candidate for acetylating both components
661 of the two-component system, which might lead to the prolonged activation of the response regulator
662 when PCE is not present anymore. PFOR, pyruvate:ferredoxin oxidoreductase; Fd, ferredoxin; ε-Nuo,
663 epsilonproteobacterial complex I; Qdh, quinol dehydrogenase; RR, response regulator; HK, histidine
664 kinase.

665

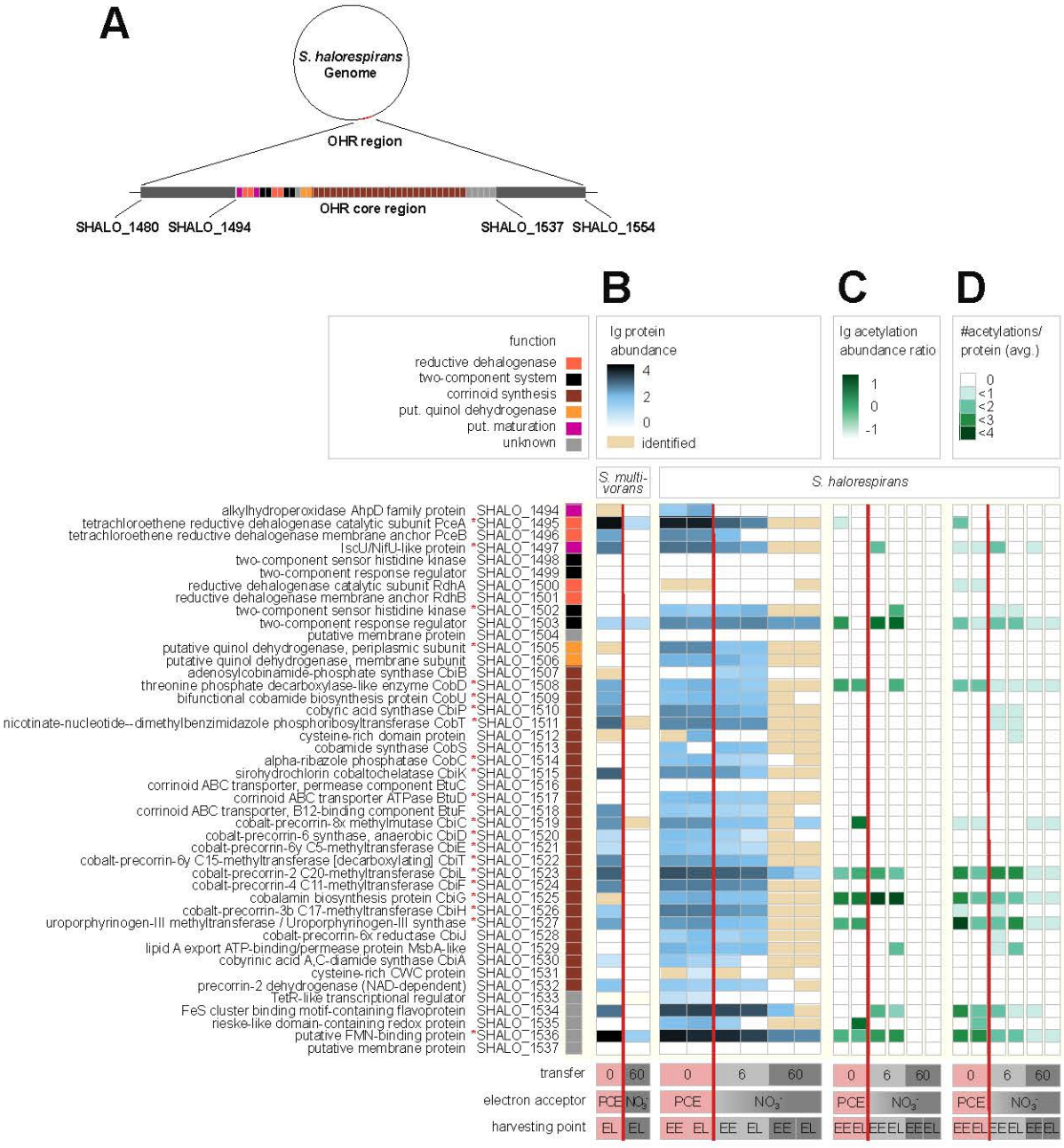

666

667 Fig. 6. The organohalide respiratory (OHR) core gene region (A), protein intensity pattern of *S.*
668 *halorespirans* and *S. multivorans* (B) and acetylome pattern (C + D) of *S. halorespirans*. Locus tags
669 and protein descriptions are given on the left of the protein intensity pattern. Colored squares adjacent
670 to the protein locus tags indicate their function in OHR. Each square of the protein intensity pattern (B)
671 corresponds to a given protein quantified (shown in blue, color code on top, normalized and
672 logarithmized average of top three peptide MS1-area as described in the methods section) or
673 identified (beige). Cultivation conditions at the bottom. Proteins with significant abundance differences
674 between any of the cultivation conditions are marked with a red asterisk (for details see Table S1).

675 Data for *S. multivorans* calculated from the dataset in [24]. (C) Acetylation of a given protein
676 quantifiable in > 50% of all replicates is marked in green. The relative acetylation intensity is provided
677 (color code on top, logarithmized top acetylated peptide area normalized to the intensity of the
678 corresponding unmodified protein. (D) Number of acetylation sites identified per protein, average of
679 three replicates. EE, early exponential phase; EL, late exponential phase; put., putative.

680

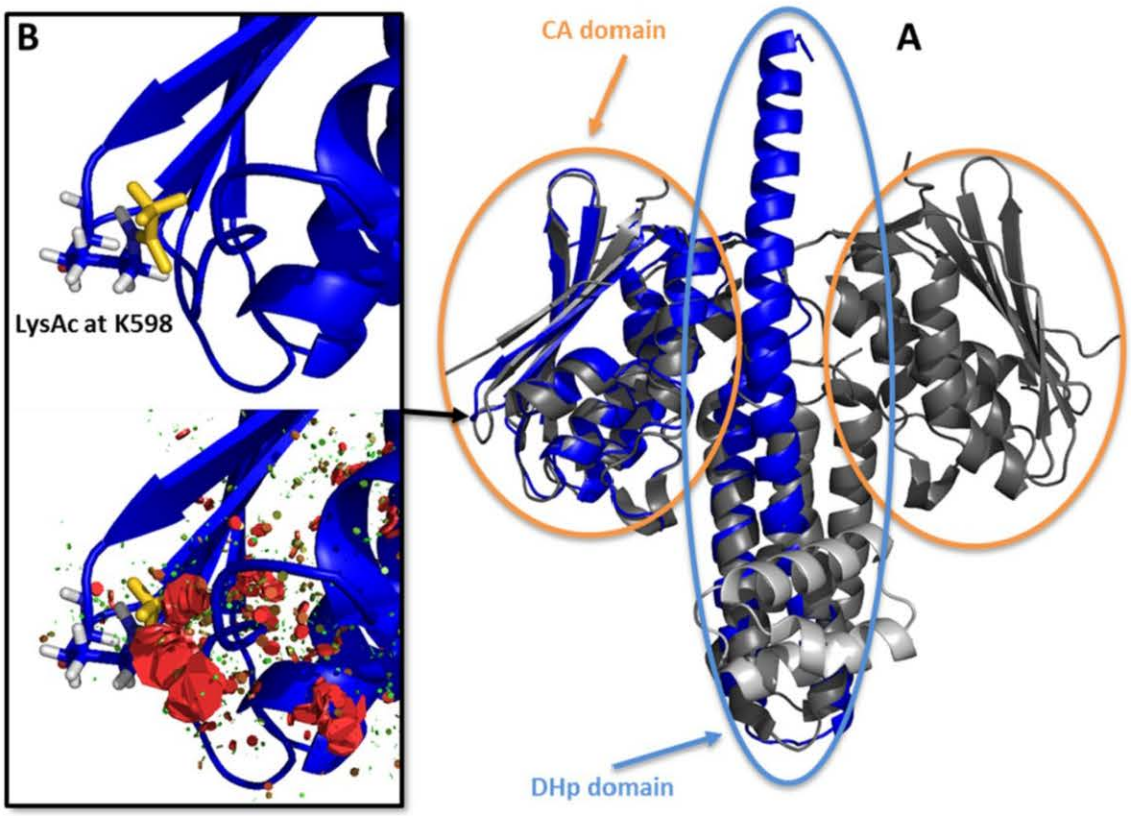

Fig. 7. (A) Predicted structural model of the catalytic core of the histidine kinase (SHALO_1501) of *S. halorespirans* (blue). Alignment with the crystal structure of the Sda/KinB catalytic core complex of *Geobacillus stearothermophilus* (PDB ID 3D36, gray). Orange circle: catalytic and ATP-binding domains (CA); blue circle: dimerization and histidine phosphotransfer (DHp) domains. (B) Part of the SHALO_1501 CA domain harboring the acetylated lysine K598. The acetylation is colored gold. In the lower panel, steric clashes based on van der Waals overlap are represented by the colored discs. The increasing size and redness of the discs correlate with stronger van der Waals strains [17].

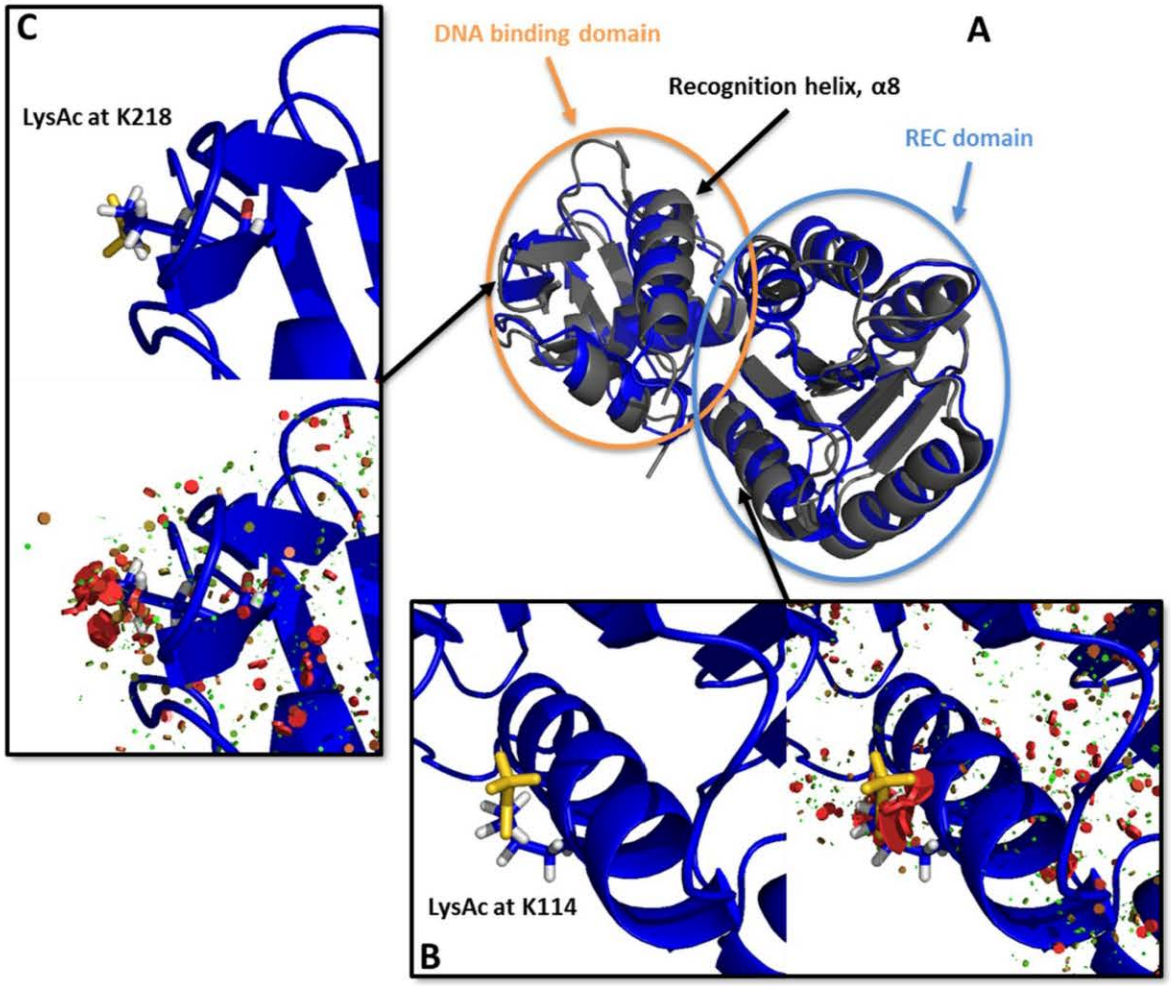

690

691 Fig. 8. (A) Predicted structural model of the response regulator (SHALO_1502) of *S. halorespirans*
692 (blue). Alignment with the crystal structure of MtrA of *Mycobacterium tuberculosis* (PDB ID 2GWR,
693 gray). Blue circle: receiver (REC) domains; orange circle: DNA-binding domains. (B) Part of the
694 SHALO_1502 DNA binding domain harboring the acetylated lysine K218 in the winged helix-turn-helix
695 (HTH) motif. (C) Part of the SHALO_1502 REC domain with the acetylated lysine K114. The
696 acetylations are colored gold. Steric clashes based on van der Waals overlap are represented by the
697 colored discs in the right or lower panel, respectively. The increasing size and redness of the discs
698 correlate with stronger van der Waals strains [17].

699